NASA TECHNICAL NOTE

NASA TN D-2333

C. 1

NASA TN D-2333

A THEORETICAL STUDY OF THE MARTIAN AND CYTHERIAN IONOSPHERES

by R. B. Norton

Prepared under NASA Order No. R-65 *by*
NATIONAL BUREAU OF STANDARDS
DEPARTMENT OF COMMERCE
for

NATIONAL AERONAUTICS AND SPACE ADMINISTRATION • WASHINGTON, D. C. • JULY 1964

A THEORETICAL STUDY OF THE MARTIAN AND CYTHERIAN IONOSPHERES

By R. B. Norton

Prepared under NASA Order No. R-65 by
NATIONAL BUREAU OF STANDARDS
DEPARTMENT OF COMMERCE

NATIONAL AERONAUTICS AND SPACE ADMINISTRATION

For sale by the Office of Technical Services, Department of Commerce,
Washington, D.C. 20230 -- Price $1.50

TABLE OF CONTENTS

		Page
1.	Introduction	1
2.	Atmospheric Theory	2
	2.1 Dissociation	3
	2.2 Diffusion and Mixing	5
	2.3 Vertical Temperature Structure	9
3.	Theory of the Ionospheric Regions	19
	3.1 Production of Electrons	19
	a. Photoionization	20
	b. Corpuscular Radiation	21
	3.2 Ionic Reactions	23
	3.3 Continuity Equation for Electrons	25
	3.4 The Terrestrial Ionosphere	26
	a. D Region	26
	b. E Region	27
	c. F1 Region	28
	d. F2 Region	29
4.	The Ionospheres of Mars and Venus	32
	4.1 Venus	33
	4.2 Mars	36
5.	Discussion	38

A THEORETICAL STUDY OF THE MARTIAN AND THE CYTHERIAN IONOSPHERES[1]

R. B. Norton

1. INTRODUCTION

We have essentially no experimental data concerning the ionospheres and very little data concerning the atmospheres of our neighboring planets Venus and Mars: the information available usually consists of equivalent temperatures at one or two atmospheric levels, the total pressure at these levels and some indication of the composition. Analysis of the spectra of the reflected sunlight from these planets indicates the presence of carbon dioxide (CO_2) and gives an estimate of the partial pressure of CO_2 and the total atmospheric pressure. Similar analysis also gives upper limits to the amount of molecular oxygen (O_2) and water vapor. Rotational structure in the absorption bands of CO_2 and infrared emission gives some indication of the temperature. These data, together with the solar constant and solar ultraviolet spectrum and with the planetary albedo, gravity, etc., may be used to construct the vertical distribution of temperature, density and composition by considering the energy balance, dissociation of molecules, and mixing and diffusion of the gases, including the escape of the particles at the top of the atmosphere.

---

[1]This work was supported by NASA Order No. R-65.

A model ionosphere can then be constructed by considering the processes of ionization, recombination, and plasma diffusion.

2. ATMOSPHERIC THEORY

In the following discussion the atmosphere has been divided into two regions, the lower and upper atmosphere. A natural boundary for this division is the mesopause which for the earth occurs at about 85 km: above this height most of the solar ultraviolet radiation (shortward of approximately 1700A) is absorbed, giving rise to the region of O_2 dissociation, the thermosphere, and the bulk of the ionosphere. Since our primary concern is here to construct model ionospheres we are mainly interested in the upper atmosphere; however, the need for boundary conditions necessitates at least some consideration of the lower regions.

The atmospheres of Mars and Venus are usually considered to consist primarily of CO_2 and molecular nitrogen (N_2). Atomic and molecular oxygen, O and O_2, are formed in the upper atmosphere by dissociating CO_2 into carbon monoxide (CO) and O and by combining some of the resulting O to form O_2. The molecules CO and N_2 have high dissociation potentials and small photodissociation cross sections and are generally not considered to be dissociated, although certainly some carbon (C) and atomic nitrogen (N) must be present in these atmospheres, particularly because of dissociative recombination of the ions CO^+ and N_2^+. After a brief discussion of dissociation and the effects of mixing and diffusion we will consider the heat balance equation.

2.1. Dissociation

Solar radiation shortward of 1690A will dissociate CO_2 while radiation either shortward of 1760A (Schumann-Runge continuum) or shortward of 2420A (Herzberg continuum) will dissociate O_2; however, the Herzberg continuum, whose cross section is of the order of 10^{-24} - 10^{-23} cm^2, will not contribute in the upper atmosphere. The various photochemical reactions to be considered and their rates are:

$CO_2 + h\nu \rightarrow CO + O$	$\sigma_1 I_1 [CO_2]$	(2-1)
$O_2 + h\nu \rightarrow O + O$	$\sigma_2 I_2 [O_2]$	(2-2)
$O + CO + M \rightarrow CO_2 + M$	$k_3 [O] [CO] [M]$	(2-3)
$O + O + M \rightarrow O_2 + M$	$k_4 [O]^2 [M]$	(2-4)
$O + CO \rightarrow CO_2 + h\nu$	$k_5 [O] [CO]$	(2-5)
$O + O \rightarrow O_2 + h\nu$	$k_6 [O]^2$	(2-6)

where [O] refers to the number density of O etc., and

k - rate coefficient

σ - average cross section for dissociation

I - dissociating solar flux

ν - wave frequency of the radiation

h - Planck's constant

M - any third body.

These reactions have been discussed by several people [cf. Bates and Witherspoon, 1952]; we will make no attempt to solve the relevant rate equations, but will either use or scale published calculations whenever possible. We will, however, need the reaction rates per particle in order to compare the photochemical time constants with those of other processes, specifically diffusion.

Particle	Reaction	Time for Association
O	(2-4)	$1/k_4$ [O] [M]
CO	(2-3)	$1/k_8$ [O] [M]
		Time for Dissociation
O_2	(2-2)	$1/\sigma_2 I_2$
CO_2	(2-1)	$1/\sigma_1 I_1$

Table 1

Although the cross section is dependent on wavelength we will use a single average value for O_2 (10^{-17} cm^{-2}) and CO_2 (5×10^{-19} cm^{-2}) [Wilkinson and Johnston, 1950; Penndorf, 1949]. According to Bates and Witherspoon [1952] and Penndorf [1949] the recombination coefficients are k_8 (5×10^{-38} cm^3 sec^{-1} $T^{\frac{1}{2}}$) and k_4 (5×10^{-34} cm^3 sec^{-1} $T^{\frac{1}{2}}$). Morgan and Schiff [1963] give 2.8×10^{-33} for k_4 at a temperature of 293°K which is consistent with the above results if the coefficient does in fact vary as $T^{\frac{1}{2}}$. It will be assumed that the same flux is responsible for dissociating CO_2 and O_2 and is given, for the earth, approximately by 6×10^{11} photons cm^{-2} sec^{-1} [Nicolet and Mange, 1954].

2.2. Diffusion and Mixing

A planetary atmosphere is in equilibrium between the pressure and gravitational forces (the centrifigal force for a rotating planet is usually included in an effective gravitational force):

$$\frac{1}{\rho}\frac{\partial P}{\partial h} + g = 0 \qquad (2\text{-}7)$$

where

ρ - mass density

P - pressure

g - acceleration of gravity

h - height above reference level

That is, the total pressure is given by the hydrostatic equation. The pressure at any point is also given by the perfect gas law:

$$P = [M]\, kT = \rho \frac{R}{\bar{M}} T \qquad (2\text{-}8)$$

where

[M] - number density

T - temperature

k - Boltzmann's constant

R - gas constant

$\bar{M}$ - mean molar weight

Combining the above two equations and integrating one obtains the barometric equation:

$$P = P_o \, e^{-\int_{h_o}^{h} \frac{dh}{H}} \tag{2-9}$$

where

$$H = \frac{RT}{Mg} \tag{2-10}$$

is the scale height and the zero subscript corresponds to the base height. The number density can be obtained by combining equations (2-8) and (2-9):

$$[M] = [M]_o \, \frac{T_o}{T} \, e^{-\int_{h_o}^{h} \frac{dh}{H}} \tag{2-11}$$

In an atmosphere containing a mixture of gases with no processes acting other than the pressure and gravitational forces the partial pressure for each gas is distributed according to equation (2-9) with a scale height corresponding to the local mean molar mass $\bar{M}$, where

$$\bar{M} = \frac{\Sigma \, n_j \, M_j}{\Sigma \, n_j} \tag{2-12}$$

where the subscript j denotes the various species of particles.

However, there are often other processes acting which vitiate the use of (2-9) with the scale height for the individual gases, but which do not proceed fast enough to invalidate the use of (2-9) with the mean molar mass. Thus, convection and winds act not fast enough to invalidate (2-9) for the total pressure, but still fast enough to overcome diffusive separation, resulting in what is called a mixed atmosphere, that is an atmosphere whose composition does not vary appreciably with height. This mixed state dominates in the lower terrestrial atmosphere, but as one proceeds upward in height an altitude is reached where diffusive separation dominates mixing. Although this transition height is very important, its determination in the terrestrial atmosphere came only through recent direct observation [Meadows and Townsend, 1960] and at this time we can hope only to make an educated guess for the other planets. A common assumption to make is that the planetary atmospheres are mixed up to the dissociation region and that in the dissociation region mixing dominates diffusion, but that photochemistry associated with dissociation dominates mixing and that above the dissociation region diffusive separation prevails.

However, we can compare the effects of photochemistry and diffusion by comparing their characteristic time constants and make the approximation that whichever process has the shorter time constant dominates and determines the distribution of the gas. To this end we might compare the time constants given in table 1 with the approximate diffusion time constant [Mange, 1957]:

$$\tau \simeq D/H^2 \qquad (2\text{-}13)$$

where D is the diffusion coefficient and is given approximately by Chapman and Cowling [1960]:

$$D = \frac{3}{8 \sigma_{12}^2 [M]} \left[\frac{kT}{2\pi} \frac{m_1 + m_2}{m_1 m_2}\right]^{\frac{1}{2}} = \frac{b}{[M]} \qquad (2\text{-}14)$$

where

σ_{12} - collision cross section

m - mass of particles

Thus by requiring that the diffusion time constant (2-13) be smaller than the oxygen association time constant (table 1), we find the condition for O to be in diffusive equilibrium as opposed to photochemical equilibrium:

$$[O]\,[M]^2 < 2 \times 10^{38} \left(\frac{100}{T}\right)^{3/2} \text{cm}^{-9} \qquad (2\text{-}15)$$

Similar conditions can be obtained for the other gases and are presented graphically in figure 1: where the lines [given by (2-15) and similar equations] separate regions of diffusive equilibrium from regions of photochemical equilibrium. The region above each line refers to smaller densities and the region of diffusive equilibrium for the indicated constituent. From this graph it is apparent that diffusion will seriously distort the photochemical profile for CO and that in all likelihood CO_2, CO and O will be in diffusive equilibrium rather than photo-

chemical equilibrium above the main dissociation region which occurs at a total density of the order of 10^{14} or less for CO_2/N_2 ratios greater than say 0.1 [cf. Shimizu, 1963]. Unless mixing is important, the bulk of the ionosphere, which occurs at densities less than 10^{12} will be in a region where diffusive separation prevails.

2.3. Vertical Temperature Structure

The vertical distribution of the atmospheric gas depends on the vertical profile of temperature which in turn depends on the detailed energy balance. The planet, obtaining almost all of its energy from the sun, is expected on the average to be in equilibrium, losing very nearly as much energy as gained during the course of a day. However, this is not to say that the temperature at any given instant is in steady state.

Although some of the solar radiant energy is absorbed directly by the atmospheric gases, most of the energy is absorbed by the planetary surface: a large fraction of the energy is then reradiated in wavelength regions readily absorbed by the gases in the lower atmosphere. This exchange of energy between the surface and the atmosphere gives rise to the greenhouse effect by increasing the surface temperature above the value for a corresponding atmosphere that is optically thin at all wavelengths.

A temperature profile can be obtained by simultaneously solving the radiative transfer equation and a heat balance equation, but such a procedure gives rise to a very complex problem. The procedure usually followed is to obtain steady state temperature profile considering only

radiative processes and then to require that the resulting atmosphere be convectively stable; if it is not, one assumes the temperature gradient to be given by the adiabatic lapse rate until a height is reached where the radiative profile gives a stable atmosphere. Vertical temperature profiles have been constructed for the lower atmospheres of Mars and Venus and we will consider the problem no further, but will use existing results.

Of the solar energy that is absorbed directly by the atmosphere, the ultraviolet and X ray radiation that ionizes and dissociates in the upper atmosphere is the most important for us, as it is this radiation that most likely supplies the energy required to maintain the thermosphere [Hunt and VanZandt, 1961]. The absorption of radiation by an atmosphere has been treated in simple form by Pedersen [1927] and Chapman [1931]. Generalizing the above mentioned work to several wavelengths and constituents and to a non-isothermal atmosphere the flux is given by:

$$I = \sum_i I_{oi} \, e^{-\tau_i \sec \chi} \tag{2-16}$$

where I_{oi} is the flux at the "top" of the atmosphere and

$$\tau_i = \sum_j \sigma_{ij} \int_h^\infty n_j \, dh \tag{2-17}$$

is the optical depth for the i'th wavelength region, σ_{ij} is the absorption cross section for the i'th wavelength and the j'th constituent and χ is the solar zenith angle. In the case of the ionizing radiation

especially below about 600A we can rewrite (2-17) by assuming that the mass absorption coefficient $\sigma_{mi} = \frac{\sigma_{ij}}{m_j}$ is the same for all constituents:

$$\tau_i \simeq \sigma_{mi} \int_h^\infty \rho \, dh \tag{2-18}$$

The absorption of energy and conversion to kinetic energy can be written:

$$G = \sum \epsilon_{ij} \, \sigma_{ij} \, n_j \, I_i \tag{2-19}$$

or again below about 600A

$$G = \sum \epsilon_{ij} \, \sigma_{mi} \, \rho \, I_i \tag{2-20}$$

where ϵ_{ij} is an efficiency factor for the conversion of radiative to kinetic energy.

In solving the heat balance equation we will find that we are able to restrict our discussion to heights above the dissociation region and since the ionizing radiation produces essentially two peaks of ionization we will consider two effective wave length regions characterized by the mass absorption cross sections $\sigma_{m2} = 2.26 \times 10^5$ cm^2 gm^{-1} (F1 region) and $\sigma_{m1} = 1.13 \times 10^4$ (E region). In order to obtain $\epsilon_{ij} \, I_i$ we will assume ϵ_{ij} is independent of the particular gas particle and will assume that the $\epsilon_i I_i$ are in the ratio of ionization produced in the two regions: thus, comparing the ionization profiles given by Norton et al. [1963] we find

that $\epsilon I_1 / \epsilon I_2$ is approximately $\frac{1}{3}$. The actual value of ϵI will be found by normalizing to the terrestrial thermospheric temperatures and extrapolating to the other planets by the inverse distance squared law.

Several people have considered the importance of radiation loss in cooling the thermosphere and Bates [1951] considered several particles that might contribute; although he found that 62 μ from the ground state of O was the most significant contributor in the terrestrial thermosphere, we must again consider the problem for the other planets especially since Chamberlain [1962] suggests that CO is the most important radiator in the Martian thermosphere. Following Bates [1951] we can write:

$$R_O \simeq \frac{h\nu_1 \, A_{12} \, [O] \, \omega_1 \, e^{-h\nu_1/kT}}{\omega_2 + \omega_1 \, e^{-h\nu/kT}} \tag{2-21}$$

$$\simeq 1.7 \, [O] \, e^{-.02/kT} \text{ erg cm}^{-3} \text{ sec}^{-1}$$

$$R_{CO}(\nu) = \epsilon \, [CO] \, [M] \, k \, e^{-h\nu/kT} \tag{2-22}$$

$$\simeq 4.3 \times 10^{-27} \, [CO] \, [M] \, e^{-.27/kT} \text{ erg cm}^{-3} \text{ sec}^{-1}$$

$$R_{CO_2} = h\nu \, [CO_2] \, [M] \, k \, e^{-h\nu/kT} \tag{2-23}$$

$$= 3.4 \times 10^{-28} \, [CO_2] \, [M] \, e^{-.085/kT} \text{ erg cm}^{-3} \text{ sec}^{-1}$$

where

A_{12} - Einstein transition coefficient (8.9×10^{-5} sec^{-1})

k - Excitation rate coefficient (10^{-14} cm^3 sec^{-1} for CO and 2.5×10^{-15} cm^3 sec^{-1} for CO_2)

R - Time rate of radiant energy emission

In order to determine which of the particles contribute most significantly to the radiative loss, ratios were formed and evaluated at 100°K and 500°K and are presented in table 2.

	100°K	500°K
R_O/R_{CO}	$8.85 \times 10^{21} \frac{[O]}{[CO]\,[M]}$	$1.3 \times 10^{11} \frac{[O]}{[CO]\,[M]}$
R_O/R_{CO_2}	$1.2 \times 10^{13} \frac{[O]}{[CO_2]\,[M]}$	$2.26 \times 10^{10} \frac{[O]}{[CO_2]\,[M]}$

Table 2

In order to illustrate the magnitudes of the ratios in table 2, we will use Chamberlain's [1962] model Martian atmosphere; the ratio R_O/R_{CO} is 7×10^7 for 100°K and 7.8 for 500°K while R_O/R_{CO_2} is 2×10^3 for 100°K and 8×10^8 for 500°K. Thus, neither CO nor CO_2 compete with O radiation, at least in the examples presented. However, at lower heights, below and in the lower dissociation region, CO_2 will become the dominant radiator. As long as we are considering the region above the dissociation level, we will assume that the radiation loss comes only from O; however, each model calculation should be checked for consistency.

Spitzer [1949] pointed out that thermal conduction could play an

important role in the thermosphere and Bates [1959] suggested that the appropriate conductivity coefficients are $k = 36\ T^{\frac{3}{4}}$ for N_2 and $56\ T^{\frac{3}{4}}$ for O. In the case of an atmosphere of several gases the effective conductivity that should be used is the average formed by weighting the separate conductivities with the appropriate number density.

The heat balance equation can now be written:

$$c_v \rho \frac{\partial T}{\partial t} = \frac{\partial}{\partial h} \left(k \frac{\partial T}{\partial h} \right) + G - R_o \qquad (2\text{-}24)$$

where c_v is the specific heat at constant volume.

In order to obtain an approximate solution for equation (2-24) we will make a number of simplifying assumptions, the first of which will be to assume steady state as at least approximately representing the actual temperature profile. We will also assume that equation (2-20) adequately represents the energy source and that the expression $\exp(-228/T)$ in the radiative loss term can be replaced with an average value. With these assumptions and by making the following transformation we will find that the solution of (2-24) can be written in terms of simple functions.

$$\frac{\partial}{\partial h} = - \sigma_m \rho \frac{\partial}{\partial \tau} \qquad (2\text{-}25)$$

Although the absorption coefficient used in the above expression is arbitrary we will use σ_{m_2} (corresponding to the F1 region peak of ionization), but will drop the subscript 2. Application of (2-25) transforms (2-24) to:

$$\sigma_m \rho \frac{\partial}{\partial \tau} (k \sigma_m \rho \frac{\partial T}{\partial \tau}) + \Sigma \sigma_{mi} \rho I_i e^{-\tau_i \sec \chi} - L_o[0] = 0 \qquad (2\text{-}26)$$

If it were not for the radiative term we could divide by ρ and greatly simplify (2-26); however, if we consider that the radiative term is only important at the lower heights we might suspect that not too great an error is made by making the oxygen density proportional to the mass density. If we denote the proportionality constant by f and substitute the expression $k = k_n T^n$ for the conductivity coefficient (2-26) can be written:

$$\frac{\partial}{\partial \tau} (\tau \frac{\partial T^n}{\partial \tau}) + \Sigma \Psi_i \frac{\sigma_{mi}}{\sigma_m} e^{-\frac{\sigma_{mi}}{\sigma m} \tau \sec \chi} - \varphi = 0 \qquad (2\text{-}27)$$

where

$$\Psi_i = \frac{\epsilon_i I_{oi} R n}{k_n M g} \qquad (2\text{-}28)$$

$$\varphi = \frac{L_o Rn f}{\sigma_m k_n Mg} \qquad (2\text{-}29)$$

and where we have used the approximate expression for the optical depth

$$\tau \simeq \sigma_m \rho H \qquad (2\text{-}30)$$

Integrating between $\tau = 0$ and τ the first integral of (2-27) is:

$$\tau \frac{\partial T^n}{\partial \tau} = \Sigma \Psi_i (e^{-\frac{\sigma_{mi}}{\sigma m} \tau \sec \chi} - 1) \cos \chi + \varphi \tau \qquad (2\text{-}31)$$

where we have taken $\tau \frac{\partial T^n}{\partial \tau} \to 0$ as $\tau \to 0$ which implies no conductive flux at the top of the atmosphere, that is no coronal conduction. Integrating between $\tau = \tau_o$ and τ the second integral is:

$$T^n = T_o{}^n + \Sigma \psi_i \cos \chi \left[Ei(- \frac{\sigma_{mi}}{\sigma_m} \tau \sec \chi) \right. \tag{2-32}$$

$$\left. - Ei(- \frac{\sigma_{mi}}{\sigma_m} \tau_o \sec \chi) + \ell n \frac{\tau_o}{\tau} \right] - \varphi[\tau_o - \tau]$$

where

$$Ei(- \chi) = - \int_{\chi}^{\infty} \frac{e^{-t}}{t} dt$$

is the exponential integral.

If boundary conditions are not available (T_o at some τ_o) then boundary conditions can be determined at the mesopause where by definition $\frac{\partial T}{\partial \tau} = 0$. Equation (2-31) gives

$$\Sigma \psi_i \left(e^{- \frac{\sigma_{mi}}{\sigma} \tau_o} - 1 \right) \cos \chi + \varphi \tau_o = 0 \tag{2-33}$$

which must be solved for τ_o. This τ_o can then be used with a model of the lower atmosphere and the relation (2-30) for the optical depth to determine the temperature. Care must be exercised in interpreting these results and one should check the validity of the various assumptions: in particular if the mesopause occurs below the height of dissociation, some compensation must be made for CO_2 radiation, the strong departure

of O from a diffusive distribution, and the solar energy deposited in the dissociation region.

An approximate expression can be obtained for the exospheric temperature by finding a solution for small optical depth and then letting the optical depth approach zero.

$$T^n(o) = T_o{}^n + \Sigma\, \psi_i \cos\chi[\ell n\, \tau_o + Ei(\frac{\sigma_{mi}}{\sigma_m}) + \Delta(\frac{\sigma_{mi}}{\sigma_m})] - \varphi\, \tau_o \qquad (2\text{-}34)$$

where

$$\Delta(\frac{\sigma_{mi}}{\sigma_m}) = \sum_{k=1}^{\infty} \frac{(-1)^{k-1}}{k(k!)} (\frac{\sigma_{mi}}{\sigma_m})^k \qquad (2\text{-}35)$$

The solution of the heat balance equation that we have obtained gives us temperature as a function of optical depth, but we will want number density as a function of optical depth and finally we will want all of these quantities as a function of height above some reference level. Recall Dalton's law: that the total pressure is the sum of the partial pressures.

$$\frac{P}{P_o} = \Sigma \frac{P_i}{P_o} = \Sigma \frac{P_{io}}{P_o} (\frac{P_1}{P_{12}})^{\frac{M_i}{M_1}} \qquad (2\text{-}36)$$

where we have normalized the equation with the total pressure at some reference level and have expressed each partial pressure in terms of the partial pressure P_1 by using equation (2-9). We could solve for P_1 in terms of P and boundary values; however, integrating (2-7) directly we

have:

$$P = \int_h^\infty \rho \, g \, dh \tag{2-37}$$

and comparing with (2-18) we see that if we take a mean value of gravity:

$$\tau \simeq \frac{\sigma_m \, P}{g} \tag{2-38}$$

Therefore we can replace P/P_o with τ/τ_o in (2-36) and solve for the partial pressure P_i as a function of τ in terms of the optical depth and partial pressures at the boundary. We are now in a position to compute density, mean molar mass and scale height as a function of optical depth and can determine the optical depth or pressure as a function of height:

$$h = h_o + \int_{P_o}^{P} H \frac{dP}{P} \simeq h_o + \int_{\tau_o}^{\tau} H \frac{d\tau}{\tau} \tag{2-39}$$

One additional problem needs some mention: that the atmosphere may, at some altitudes, become optically thick to the oxygen emission [Bates, 1951] which would inhibit the cooling of the atmosphere. To include this effect in an exact manner in the present development would cause excessive difficulties and seems unwarranted; we can take this effect into account in an approximate way by treating f as a disposable parameter. We can then determine f and ϵI by using the gradient at the lower boundary and the exospheric temperature and solving equations (2-31) and (2-34).

The above procedure has been applied to the terrestrial atmosphere

and the resulting temperatures are shown in figure 2. The values of ϵI are smaller than given by a similar study by Hunt and VanZandt [1961], but can be explained in terms of the different conductivities used. The agreement between this model and CIRA [1961] is not particularly good at the lower heights, but should be adequate. These values of ϵI can be extrapolated to the other planets by using the inverse squared distance attenuation law. The f value obtained in the above analysis was about 1.0, which seems reasonable.

3. THEORY OF THE IONOSPHERIC REGIONS

Our approach to the theory of planetary ionospheres will be to review the theory of the terrestrial ionospheric regions and then to apply this theory, with whatever necessary modifications, to the other planets. Although the division of the terrestrial ionosphere into regions was originally made according to the appearance on ionograms (radar reflection records) this same division can now be made according to the important processes. Therefore, before we consider the specific ionospheric regions we will first discuss some important processes: the production of electrons, the exchange and recombination reactions and finally the diffusion of an electron-ion gas through the neutral gas.

3.1. Production of Electrons

Photoionization by solar X-ray and ultraviolet radiation seems adequate to explain most of the ionization in the terrestrial ionosphere

and will be discussed first; corpuscular ionization will then be discussed.

a. Photoionization

The first treatment of the problem of photoionization in the upper atmosphere was that of Pedersen [1927] although the work more familiar to aeronomists is that of Chapman [1931]. The above treatments can easily be generalized to several constituents, several wavelengths and non-isothermal atmosphere. The flux as a function of optical depth τ_i is given by equation (2-16).

The rate of producing electrons by ionizing the j'th constituent is then

$$q_{ij} = \sigma_{ij}\ \eta_{ij}\ N_j\ I_j \simeq \sigma_{mi}\ \eta_{ij}\ \rho_i\ I_i \qquad (3\text{-}1)$$

and the total rate is

$$q = \sum_{ij} q_{ij} \qquad (3\text{-}2)$$

where

η_{ij} - Ionization efficiency

Estimates of the solar EUV flux that are now available [Hinteregger, 1961; Kreplin, 1961; Hall et al., 1962] allow photoionization rates to

be estimated [Norton et al., 1963].

b. Corpuscular Radiation

Energetic particles as they penetrate an atmosphere lose energy in various types of collisions, some of which produce ionization. If W is the average energy required to form one electron-ion pair, then the energy ΔE deposited per unit path length ΔS divided by W gives the average number of electron-ion pairs N_q formed per unit path length: that is

$$N_q = \frac{1}{W} \frac{\partial E}{\partial S} \tag{3-3}$$

If we consider a monoenergetic and monodirectional flux F of particles of initial energy E_o (initial residual range r_o) incident on the atmosphere at an angle θ from the vertical, then we can write the production rate per unit volume

$$q = F\ p \frac{\partial r}{\partial S} = F_p \frac{[M]}{[M]_{stp}} \tag{3-4}$$

where

$$r = r_o - \int_h^\infty \frac{[M]\ dh'\ \sec\theta}{[M]_{stp}} \tag{3-5}$$

$[M]_{stp}$ is the total density at standard temperature and pressure and

$$p = \frac{1}{W} \frac{\partial E}{\partial r} \tag{3-6}$$

gives the Bragg curve. For low energy (small residual range $r < .025$) the Bragg curve can be approximated by:

$$p = p_o r \tag{3-7}$$

and the ionization rate becomes:

$$q = F\ p_o \frac{[M]}{[M]_{stp}} \left(r_o - \frac{[M]\ H}{[M]_{stp}} \sec \theta\right) \tag{3-8}$$

Some of the properties of this equation can be determined most simply by considering an isothermal atmosphere. The usual techniques of calculus give for the height h_p of maximum rate:

$$h_p = h_o + H\ \ell n\ 2 \sec \theta \tag{3-9}$$

and thus the maximum rate q_p is:

$$q_p = \frac{F\ p_o\ r_o^2}{4H} \cos \theta \tag{3-10}$$

where h_o is defined by:

$$r_o = \int_{h_o}^{\infty} \frac{[M]\ dh'}{[M]_{stp}} \sec \theta \tag{3-11}$$

The Mariner II data (IGY Bulletin No. 73) suggests that during quiet conditions the energy flux contained in the solar wind is of the

order of .1 erg cm^{-2} sec^{-1}, but that during active conditions the flux can be in excess of 1 erg cm^{-2} sec^{-1}. The protons carry most of this energy so that if we assume that these particles are not inhibited by a planetary magnetic field, we can use the previously derived formula to estimate the peak production. If, for storm conditions, we consider 10 kev protons with a total flux of 10^8 cm^{-2} sec^{-1} we obtain a peak rate of 2×10^3 cm^{-3} sec^{-1} occurring between the E and F1 photoionization peaks: for quiet conditions we obtain 40 cm^{-3} sec^{-1} occurring somewhat above the F1 peak. A similar calculation for photoionization gives 4×10^3 cm^{-3} sec^{-1} for the F1 ionization peak which implies that during disturbed conditions corpuscular ionization will enhance the F1 layer density by only 25% and that during quiet conditions corpuscular ionization is negligible: therefore, we will not need to consider this radiation further. The above calculations apply only in the event that the planets do not have a magnetic field. If Mars or Venus does have a significant magnetic field then corpuscular radiation might become important, especially at night and in polar regions (assuming a dipole field).

3.2. Ionic Reactions

Recombination loss of electrons is an important process that must be considered in any ionospheric theory. The two main loss processes are dissociative and radiative recombination:

$$xy^+ + e \rightarrow x + y \qquad \alpha_{52} [xy^+] N_e \qquad (3\text{-}12)$$

$$xy^+ + e \rightarrow xy + h\nu \qquad \alpha_{53}\,[xy^+]\,N_e \qquad (3\text{-}13)$$

It is important to realize that dissociative recombination is much faster than radiative recombination, the rate coefficients being 10^{-6} - 10^{-9} cm^3 sec^{-1} and about 10^{-12} cm^3 sec^{-1} respectively. The atomic ions recombine radiatively unless they can undergo reactions such as atom-ion and charge exchange:

$$x^+ + yz \rightarrow xy^+ + z \qquad \gamma_{54}\,[yz]\,[x^+] \qquad (3\text{-}14)$$

$$x^+ + yz \rightarrow yz^+ + x \qquad \gamma_{55}\,[yz]\,[x^+] \qquad (3\text{-}15)$$

followed by dissociative recombination of the resulting molecular ion. The exchange coefficients are usually of the order of 10^{-10} - 10^{-12} cm^3 sec^{-1}; however, the sequence of an exchange reaction and dissociative recombination is often much faster than radiative recombination.

In addition to the processes thus far mentioned, electron attachment can also become important, but unless a particle of unusually high electron affinity is present this process is slow except at pressures to be found in the lowest ionosphere.

$$x + e + M \rightarrow x^- + n \qquad k_{56}\,[x^-][N_e][M] \qquad (3\text{-}16)$$

$$x^- + y^+ \rightarrow x + y \qquad \alpha_{57}\,[x^-][y^+] \qquad (3\text{-}17)$$

With the formation of negative ions one must also consider the possibility of collisional detachment, but this process does not usually compete with photodetachment.

$$x^- + M \rightarrow x + M + e \qquad k_{58}\,[x^-][M] \qquad (3\text{-}18)$$

$$x^- + h\nu \rightarrow x + e \qquad \sigma_{59}\,I\,[x^-] \qquad (3\text{-}19)$$

3.3. Continuity Equation for Electrons

As the neutral gas becomes sufficiently tenuous, ambipolar diffusion of electrons and ions will dominate the other processes; the application of plasma diffusion to the ionosphere was first treated in detail by Ferraro [1945].

The effect of diffusion on the electrons is accounted for by including a term of the form Div $(N_e U)$ in the continuity equation:

$$\frac{\partial N_e}{\partial t} + \text{Div}\,(N_e U) = Q - L \qquad (3\text{-}20)$$

where

Q - rate of formation of electrons

L - rate of recombination of attachment of electrons

U - diffusion velocity

Similar equations can be written for the ions.

The simultaneous inclusion of all the previously discussed processes would pose an extremely complex mathematical problem; fortunately, the processes are strongly height dependent, with each process being important only in a restricted height region, thus allowing the problem to be greatly simplified. The next section will discuss the terrestrial ionospheric layers and the corresponding approximations.

3.4. The Terrestrial Ionosphere

A vertical profile of the electron density in the terrestrial ionosphere reveals considerable structure that results in the ionosphere being divided into regions: D, E, F1 and F2 in order of increasing height. Each region corresponds to different production and loss mechanisms. The ideas outlined below explain many, but not all, of the features of the terrestrial ionosphere: most striking of the unexplained features are the seasonal and annual variations, the nighttime behavior, and the magnetic field control of the latitudinal variation of the F2 layer.

a. D Region

Although nearest to the earth's surface, the D region is in some respects the least understood; certainly there is less meaningful data for this region than for any other. According to current theory [Nicolet and Aiken, 1960], the upper D region is formed by ionization of NO by solar HLyα, while the lower region is formed by ionization of all constituents by cosmic rays and solar X rays; although the importance

of the latter processes is subject to some debate for quiet conditions, X rays certainly are important during solar flares [cf. Kreplin et al., 1962; Chilton et al., 1963].

The pressures are sufficiently large throughout most of this region that the attachment rate of electrons, especially to O_2, is appreciable; in fact, if it were not for this attachment, the density of free electrons would be sufficiently great at the lower heights to cause severe absorption of radio waves.

b. E Region

The E region is likely formed primarily by ionization of all constituents by solar X rays between about 40 and 100A [Hulburt, 1938; Norton et al., 1963] although radiation between 912 and 1030A must contribute some ionization and has been suggested as the primary source [Wulf and Deming, 1938; Watanabe and Hinteregger, 1962]. The ions in this region must undergo some exchange reactions since the dominant ion is NO^+ [cf. Taylor and Brinton, 1961]; however, the only exchange reaction leading to NO^+ that is accepted by most aeronomists is:

$$O^+ + N_2 \rightarrow NO^+ + N \qquad \gamma_{6o}\,[O^+][N_2] \qquad (3\text{-}21)$$

It has been argued by Norton et al. [1963] that some other reaction must also be operative in the E and F1 regions and they suggested the reaction:

$$N_2^+ + O \rightarrow NO^+ + N \qquad \gamma_{61}\,[N_2^+][O] \qquad (3\text{-}22)$$

Regardless of details, both theory and observation suggest that the E region density is given reasonably well by:

$$\frac{\partial N_e}{\partial t} = q - \alpha_{eff} N_e^2 \qquad (3\text{-}23)$$

where α_{eff} is the effective recombination coefficient.

The actual loss of electrons proceeds via dissociative recombinations:

$$[NO^+] + e \rightarrow N + O \qquad \alpha_{63} [NO^+] N_e \qquad (3\text{-}24)$$

$$[N_2^+] + e \rightarrow N + N \qquad \alpha_{64} [N_2^+] N_e \qquad (3\text{-}25)$$

$$[O_2^+] + e \rightarrow O + O \qquad \alpha_{65} [O_2^+] N_e \qquad (3\text{-}26)$$

Both ionospheric observation and laboratory measurements suggest that the effective recombination coefficient is of the order of 10^{-7} cm^3 sec^{-1} in the E region. While, some of the older ionospheric work, particularly eclipse analyses, suggested 10^{-8} cm^3 sec^{-1}, it should be kept in mind that this work assumed no solar limb brightening which, to the contrary, has now been established [Kreplin, 1961].

c. F1 Region

The F1 region is accounted for by the ionization of O and N_2 by solar radiation between 100 and 900A and with the same exchange and re-

combination reactions operative as in the E region. A ledge corresponding to the peak of ionization rate may occur in this region depending on whether dissociative recombination or atom-ion exchange is the faster reaction: if atom-ion exchange is the faster then a ledge may occur.

Hirsh [1959] has given the approximate solution for the electron density in this region:

$$\frac{\partial N_e}{\partial t} = q - \frac{\beta\, \alpha_{eff}\, N_e^2}{\beta + \alpha_{eff}\, N_e} \qquad (3\text{-}27)$$

where

$$\beta \simeq \gamma_{60}\, [N_2] \qquad (3\text{-}28)$$

This equation is only approximate since (3-22) or some equivalent reaction is not included, but should be sufficient for our purpose. The α_{eff} in the F1 region is somewhat smaller than in the E region; Norton et al. [1963] suggested a T^{-1} dependence for the recombination coefficient.

d. F2 Region

The F2 region is caused by the same ionizing radiation as is the F1 region; the electron density increases with increasing height above the ionization peak because the loss rate decreases faster than the ionization rate with increasing height. Contrary to what is occasionally stated, photochemistry will give an actual peak without the aid of diffusion, but not a steady state peak. However, diffusion does play a role,

especially above the F2 peak where diffusive equilibrium is obtained and also in lowering the height of the peak. The equation describing the behavior of the electron density can be obtained by requiring that $\alpha_{eff} N_e > \beta$ in (3-27) and by including diffusion

$$\frac{\partial N_e}{\partial t} = q - \beta N_e - \text{Div}\,(N_e U) \qquad (3\text{-}29)$$

This equation has been discussed by many workers, but for our purposes the scaling laws suggested by the work of Rishbeth and Barron [1960] will be adequate. These laws state that the F2 peak occurs at that height where the diffusion time is nearly equal to the recombination time:

$$\frac{D_{12}}{H^2} \simeq \beta \qquad (3\text{-}30)$$

(where $D_{12} = 2D$ is the ambipolar diffusion coefficient) and that the electron density at this height is given approximately by the steady state photochemical value:

$$N_e \simeq \frac{q}{\beta} \qquad (3\text{-}31)$$

Although the above equations can be solved graphically, we will find approximate expressions more convenient. The total density in the diffusion coefficient causes (3-30) to be transcendental; however, if we assume that, at the F2 peak, the atomic oxygen density exceeds the molecular nitrogen density we obtain the equation for the optical depth at the

F2 peak:

$$\frac{\tau}{\tau_o} \simeq \left[\frac{b}{\gamma}\left(\frac{\bar{M}g}{RT_o}\right)^2 \frac{1}{[N_2]_o\,[O]_o}\right]^{\frac{3}{11}} \tag{3-32}$$

The zero subscripts refer to some boundary height that is arbitrary except that the height must fall in the region where diffusive separation prevails. The fact that some of the quantities under the bracket on the rhs of (3-32) depend on height or optical depth should present no problem in practice since this dependence is in general rather weak. Now that we have the height of the F2 peak we can evaluate (3-31) to find the peak density:

$$N_e \simeq \frac{\eta\sigma I}{\gamma}\frac{[O]_o}{[N_2]_o}\left(\frac{\tau}{\tau_o}\right)^{\frac{3}{4}}$$

$$= \eta\sigma I\, \frac{b^{\frac{3}{11}}}{\gamma^{\frac{8}{11}}}\, \frac{[O]_o^{\frac{8}{11}}}{[N_2]_o^{\frac{14}{11}}}\left(\frac{\bar{M}g}{RT_o}\right)^{\frac{6}{11}} \tag{3-33}$$

Since γ is usually considered to be independent of temperature (more because of the lack of data than for any other reason) and since (2-14) gives b as proportional to $T^{\frac{1}{2}}$, we see that the F2 peak density is essentially independent of temperature [Rishbeth, 1964]. Therefore, if we are given certain boundary conditions and the solar ionizing flux, then we can compare the F2 density for various model atmospheres and various planets. We must stress particularly that the above equations are applicable only when atomic oxygen is the dominant constituent near the F2 peak.

Helium and hydrogen ions become important a few scale heights above the F2 peak; helium at about 500-600 km and hydrogen at about 3000 km However, these light ions will probably not be as significant on Mars and Venus as on earth, unless the martian and cytherian exospheric temperatures are quite different than those derived in the following sections.

4. THE IONOSPHERES OF MARS AND VENUS

We will now apply the formulae to construct model ionospheres for Mars and Venus. However, before proceeding we shall consider the possible limits to the maximum electron density; the lower limit is given by considering the ionosphere to be entirely molecular with the ions recombining by dissociative recombination and the upper limit is given by considering the ionosphere to be entirely atomic with the ions recombining by radiative recombination. Using Chapman's [1931] equation for the peak ionization rate and considering the steady state solution of (3-23) we obtain the approximate expression for the maximum electron density:

$$N_e \simeq \sqrt{\frac{\eta I}{e\, \alpha_{eff}\, H}} \qquad (4\text{-}1)$$

This equation applies equally well to either limit, but with different values of the recombination coefficient. Since the ratio of dissociative to radiative recombination rate coefficients is about 10^5 the ratio of the limits of the maximum density is about 3×10^2 (i.e. square root of the ratio of rate coefficients) and the ratio of the corresponding maximum plasma frequency is about 17 (i.e. fourth root of the ratio of

rate coefficients). Both dissociative and radiative recombination coefficients are likely to vary inversely with temperature [cf. Bates and Dalgarno, 1962]; although the exact variation is uncertain, the variation is likely to be between $T^{-\frac{1}{2}}$ and $T^{-\frac{3}{2}}$. Therefore, since H varies as T, the electron density given by (4-1) will be nearly independent of temperature. Although the rate coefficients also depend on the particles involved in the recombination process, we will scale the terrestrial F1 peak density according to the inverse squared distance attenuation of the solar ionizing flux in order to obtain the lower limit to the maximum electron density. The upper limit to the maximum density is approximately 3×10^2 greater than the lower limit. These limits apply to the sunlit side of the planet and for "overhead" sun.

4.1. Venus

Venus is in a nearly circular orbit located at 0.72 AU from the sun and has a sidereal period of 224.7 days; the orientation of its rotation axis and the period of rotation is not known, although estimates of the rotation period vary between a few days to many weeks up to the sidereal period. The diameter and surface gravity are nearly the same as for the earth; 6100 km and about 880 cm sec^{-2} respectively. Kaplan [1961] gives the composition of the atmosphere as 15% CO_2 with the balance made up of essentially all N_2 and a cloud top pressure of 90 mb. An estimate of the pressure (2.6 ± 0.13 mb), scale height (6.8 ± 0.2 km) and scale height gradient (.01 ± 002) some 55 ± 8 km above the cloud top was obtained by de Vaucouleurs and Menzel [1960] from the Regulus occultation data.

Combining the occultation data with equation (2-10) we find that the temperature at the occultation level is:

$$T \simeq 7.2\ \bar{M}^{\circ}K \qquad (4\text{-}2)$$

If we also use the perfect gas law (2-8) with the pressure at the occultation level and (4-2) we find for the total number density at this level:

$$[M] \simeq 2.3 \times 10^{15}\ \frac{1}{\bar{M}} \qquad (4\text{-}3)$$

Now for a CO_2 to N_2 ratio of .15/.85 we find in the absence of dissociation that $\bar{M} = 30.4$ and for total dissociation, but no diffusion, that $\bar{M} = 26.4$. Shimizu [1963] in a study of the dissociation on Venus gives for the above composition, graphs from which one can determine that at the peak of the O layer the total density is about 1.2×10^{14} cm^{-3}.

If the occultation level is below the O peak then from (4-3) we find that $(2.26 \times 10^{15}/\bar{M}) > 1.2 \times 10^{14}$ or that $\bar{M} < 19$ while if the occultation level is above the O peak we find that $(2.26 \times 10^{15}/\bar{M}) < 1.2 \times 10^{14}$ or $\bar{M} > 19$; clearly the occultation level is above the O peak. Therefore, assuming total dissociation and no appreciable diffusion we find for the occultation level a temperature of 190°K and a total number density of 8.6×10^{13} cm^{-3}: the densities of N_2, O, and CO are 6.4×10^{13}, and 1.1×10^{13} cm^{-3} respectively.

A comparison of these numbers with figure 1 indicates that O should

be in photochemical equilibrium up to two or more scale heights above the occultation level; we will therefore assume that diffusive separation begins at 2.3 scale heights above the occultation level. The densities at this new level are then just a factor of 10 less than at the occultation level and the temperature is about 205°K (assuming a constant scale height gradient of 0.01 given by the occultation data).

The numbers we have obtained for 2.3 scale heights above the occultation level are very similar to the numbers encountered at 100 km in the terrestrial atmosphere and we will thus apply our thermospheric equations directly, changing only ϵI by the inverse squared distance law, giving 0.87 erg cm^{-2} sec^{-1} for sunspot minimum and 1.65 erg cm^{-2} sec^{-1} for sunspot maximum. The resulting temperature profiles, displayed in figure 3, indicate a rather high exospheric temperature; the sunspot maximum temperature is too high since at such high temperatures Spitzer's [1949] theory of exospheric particle escape would suggest that the atmosphere would have escaped. Other processes must be invoked to reduce the temperature; in particular convective transport of heat to the dark side of the planet, but the inclusion of additional processes must await a more detailed study. The corresponding neutral densities are presented in figure 4 and were used to compute the mean molar weight, scale height and optical depth (figure 5) as a function of height. Finally, the ionizing flux observed in the terrestrial atmosphere were extrapolated to the distance of Venus, ionization rates computed (figure 6) and a model ionosphere constructed (figure 7). As should be expected the cytherian and terrestrial ionospheres are similar, but with larger densities on

Venus: the maximum density for Venus being 1.2×10^6 and 3.9×10^6 cm^{-3} for sunspot minimum and maximum respectively. The height of the F2 peak is probably unrealistically high because of the extreme temperatures.

Using the procedure outlined following equation (4-1), we can determine the limits to the maximum electron density to be approximately 2.5×10^5 to 5×10^7 cm^{-3} for sunspot minimum and 5×10^5 to 10^8 cm^{-3} for sunspot maximum.

According to Shimizu [1963] a layer of O_2 is formed with a peak density of about 10^{13} cm^{-3} at a total density in excess of 10^{14} cm^{-3}. Solar HLyα will ionize the O_2 to form a layer of free electrons where the total neutral density may be sufficiently high to cause absorption of radio waves.

D region electron density is likely to be larger on Venus than on earth for two reasons: the enhancement of solar ionizing flux and the lack of attachment of electrons to O_2. The larger electron density in this region may mean significant radio wave absorption.

4.2. Mars

Mars is in an eliptic orbit (eccentricity .093) whose mean distance from the sun is 1.52 AU and whose period is about 687 days; the rotation axis is tilted 24.8° to its orbit and the rotation period is approximately 24 hr and 37 min. The martian diameter and surface gravity are about 3400 km and about 365 cm sec^{-2} respectively. de Vaucoulers [1959] summarizes our knowledge of the martian atmosphere and gives 85 mb for the surface pressure, 230-300°K for the surface temperature and about 2% CO_2,

4% A and 94% N_2 for the composition. However, more recent data suggest a surface pressure of about 25 ± 15 mb corresponding to 4^{-1}_{+2} mb CO_2 [Spinrad et al., 1964].

A model ionosphere has been developed by Norton [1963] and will be just summarized here. This model ionosphere was based on the atmospheric models developed by Goody [1957] and Chamberlain [1962] which used the older estimates of composition, i.e. 2% CO_2. The temperature and density profiles are presented in figures 8 and 9 respectively while the ionization rates and electron density are presented in figures 10 and 11 respectively. The main features of the ionosphere are the magnitude of the maximum electron density (about 2×10^5 cm^{-3} sec^{-1}) and the presence of a significant amount of ionization occurring at total neutral densities that could lead to significant absorption of radio waves [Chamberlain, 1962].

Again using the procedure following equation (4-1), we estimate the limits to the maximum electron density to be approximately 10^5 to 2×10^7 cm^{-3} for sunspot minimum and 2×10^5 to 4×10^7 for sunspot maximum.

As we have seen in a previous section the main radiative loss comes from atomic oxygen emission; however, Chamberlain in the construction of his model atmosphere used CO emission only. We have recomputed the exospheric temperature using equation (2-34); the temperature for sunspot minimum is 800°K and for sunspot maximum 1760°K. The extrapolated values of ϵI are .22 and .41 for sunspot minimum and maximum respectively and the value of f used was .01 (the density of O at the boundary was similar to that at 100 km on earth, but the total density was ten times

greater). Chamberlain's atmosphere is then quite acceptable for an average sunspot number as was assumed in the construction of the model ionosphere.

The more recent estimates of composition present a more serious problem, as the ratio of O to N_2 would now be larger leading to the possibility of a more pronounced F2 layer which could have a maximum density comparable to the terrestrial F2 maximum, particularly in the case of 60% CO_2. If we use the mean composition given by Spinrad et al. [1964] and use equation (3-33) we can estimate the martian F2 electron density to be about 0.3 of the terrestrial F2 density; that is, 1.2×10^5 cm^{-3} at sunspot minimum and 4.5×10^5 at sunspot maximum.

5. DISCUSSION

In this section we will summarize the main conclusions reached in the previous sections, particularly the limits placed on the possible maximum daytime electron densities to be expected on Mars and Venus. We will then conclude with a brief comparison with some other studies of planetary ionospheres.

The martian thermospheric temperatures were estimated to be very similar to the corresponding terrestrial temperatures, 800°K for sunspot minimum and 1800°K for sunspot maximum; the sunspot maximum temperature may cause excessive loss of atmospheric gases [Spitzer, 1952]. On the other hand, the cytherian temperatures are considerably greater than the corresponding terrestrial temperatures, 1800°K for sunspot minimum and 4000°K for sunspot maximum; loss of atmospheric gases will be a serious

problem and other energy loss processes must be investigated in order to reduce the temperatures. Fortunately, most of the ionospheric results are not sensitive to the temperature structure. An exception is the geometric height of the ionosphere above the planets surface; the estimated height of the cytherian ionosphere is likely to be too great, especially for sunspot maximum.

Mars (maximum electron density cm^{-3})

	lower limit	model (16% CO_2)	upper limit
sunspot minimum	10^5	1.2×10^5	2×10^7
sunspot maximum	2×10^5	4.5×10^5	4×10^7

Venus (maximum electron density cm^{-3})

	lower limit	model (15% CO_2)	upper limit
sunspot minimum	2.5×10^5	1.2×10^6	5×10^7
sunspot maximum	5×10^5	3.9×10^6	10^8

Table 3

Both the martian and cytherian D regions may be enhanced; the former because of the lack of attachment of electrons to O_2, the latter for the same reason and also because of the greater flux density of solar radiation. There is, however, the possibility of some other particle taking the place of O_2. There is a narrow ledge of O_2 in the upper D region which will be ionized by solar HLyα. The net result of the above

discussion is that the martian and cytherian D regions may be capable of attenuating radio waves to a greater extent than does the terrestrial D region.

Chamberlain [1962] constructed a model martian ionosphere based on an atmosphere containing 2% CO_2 with the balance being N_2. His estimate of a maximum electron density of 10^5 cm^{-3} is consistent with an ionosphere containing mostly molecular ions and is thus near the lower limit, see table 3. However, Chamberlain's conclusion that CO emission is the most important source of radiative energy loss in the thermosphere was not substantiated in this study; using Chamberlain's atmosphere and Bate's [1951] rate equations and coefficients, we found that the rate of energy lost from CO was never more than 0.15 of the energy lost from O. Nevertheless, we found that Chamberlain's model was adequate for an average sunspot number.

Yanow [1961] also has constructed a model martian atmosphere and ionosphere; unfortunately he ignored some of the most important processes in the construction of his models. For example, he ignored thermal conduction and radiative loss in computing his temperature profile; for that matter no mention was made of any energy loss processes. He also ignored exchange reactions between N^+ and oxygen, which would very likely determine the effective loss rate, if indeed atomic nitrogen were as abundant as Yanow predicts.

Danilov [1963] constructed model ionospheres for Mars and Venus, but makes no real attempt to construct model atmospheres; upper atmosphere conditions are estimated by extrapolating lower atmospheric con-

ditions ignoring, for example, photodissociation, diffusive separation, and the higher temperatures usually found in the thermosphere. Danilov assumes that the atmosphere of Mars is entirely N_2 and the atmosphere of Venus to be entirely CO_2. Some of the reactions that Danilov proposes are endothermic:

$$N^+ + N_2 \rightarrow N_2^+ + N \qquad \text{for Mars and}$$

$$O^+ + CO_2 \rightarrow CO^+ + O \qquad \text{for Venus.}$$

Nevertheless, his estimates of 10^5 cm^{-3} for Mars and 10^6 cm^{-3} for Venus are not greatly different from the model calculations presented in table 3.

As a final word it must be pointed out that most of the previous work is based on an assumed composition of CO_2 and N_2 and that while CO_2 has been detected in the atmospheres of both Mars and Venus the observational evidence for N_2 is slight. Moreover, even for the earth, where the composition in the lower atmosphere is known precisely, it is not yet possible to construct an a priori model of the ionosphere.

6. ACKNOWLEDGEMENTS

The author gratefully acknowledges helpful discussions with Dr. T. E. VanZandt. This work was supported by NASA Order No. R-65.

7. REFERENCES

Bates, D. R., Proc. Phys. Soc., B64, 805 (1951).

Bates, D. R., Proc. Roy. Soc., A253, 459 (1959).

Bates, D. R., and A. Dalgarno, Atomic and Molecular Processes, 245, D. R. Bates, ed., Academic (1962).

Bates, D. R., and A. E. Witherspoon, Mon. Not . R. Astron. Soc., 112, 101 (1952).

Chamberlain, J., Astrophys. J., 136, 582 (1962).

Chapman, S., Proc. Phys. Soc., 43, 26 (1931).

Chapman, S., and T. G. Cowling, The Mathematical Theory of Non Uniform Gases, Cambridge University, 2nd Edition (1960).

Chilton, C. J., F. K. Steele, and R. B. Norton, J. Geophys. Res., 68, 5421 (1963).

Danilov, A. D., Space Research III, 1026, W. Priester, ed., North-Holland, Amsterdam (1963).

de Vaucouleurs, G., J. Geophys. Res., 64, 1739 (1959).

de Vaucouleurs, G., and D. H. Menzel, Nature, 188, 28 (1960).

Ferraro, V. C. A., Terrest. Mag. Atmos. Elec., 50, 215 (1945).

Goody, R. M., Weather, 12, 3 (1957).

Hall, L. A., K. R. Damon, and H. E. Hinteregger, Space Research III, 745, W. Priester, ed., North-Holland, Amsterdam (1961).

Hinteregger, J. Geophys. Res., 66, 2367 (1961).

Hirsh, A. J., J. Atmos. Terrest. Phys., 17, 86 (1959).

Hulburt, E. O., Phys. Rev., 53, 344 (1938).

Hunt, D. C., and T. E. VanZandt, J. Geophys. Res., 66, 1673 (1961).

IGY Bulletin No. 73, Trans. Amer. Geophys. Union, 44, 783 (1963).

Kaplan, L. D., Planetary Space Sci., 8, 23 (1961).

Kreplin, R. W., Ann. Geophys., 17, 151 (1961).

Kreplin, R. W., T. A. Chubb, and H. Friedman, J. Geophys. Res., 67, 2231, (1962).

Meadows, E. B., and J. W. Townsend, Space Research I, 175, Kallmann-Bijl ed., North-Holland, Amsterdam (1960).

Morgan, J. E., and H. I. Schiff, J. Chem. Phys., 38, 1495 (1963).

Nicolet, M., and A. C. Aiken, J. Geophys. Res., 65, 1469 (1960).

Nicolet, M., and P. Mange, J. Geophys. Res., 59, 15 (1954).

Norton, R. B., Advances in the Astronautical Sciences, Vol. 15, G. W. Morgenthaler, ed., p. 533 (1963).

Norton, R. B., T. E. VanZandt, and J. S. Denison, Proc. Int. Conf. Iono., J. A. Ratcliffe, ed., Institute of Physics and Physical Society, London (1963).

Pedersen, P. O., The Propagation of Radio Waves Along the Surface of the Earth and in the Atmosphere, Copenhagen (1927).

Penndorf, R., J. Geophys. Res., 54, 7 (1949).

Rishbeth, H., J. Atmos. Terrest. Phys., in press (1964).

Rishbeth, H., and D. W. Barron, J. Atmos. Terrest. Phys., 18, 234 (1960).

Shimizu, M., Planetary Space Sci., 11, 269 (1963).

Spinrad, H., G. Munch, and L. D. Kaplan, Astrophys. J., 139, 1 (1964).

Spitzer, L., The Atmospheres of the Earth and Planets, G. P. Kuiper, ed., University of Chicago, 2nd Edition, p. 211 (1952).

Taylor, H. A., and H. C. Brinton, J. Geophys. Res., 66, 2587 (1961).

Watanabe, K., and H. E. Hinteregger, J. Geophys. Res., 67, (1962).

Wilkinson, P. G., and H. J. Johnstone, Phys. Rev., 18, 190 (1950).

Wulf, O. R., and L. S. Deming, Terrest. Mag. Atmos. Elec., 43, 283 (1938).

Yanow, G., Engineering paper No. 974, Douglas Aircraft Company (1961).

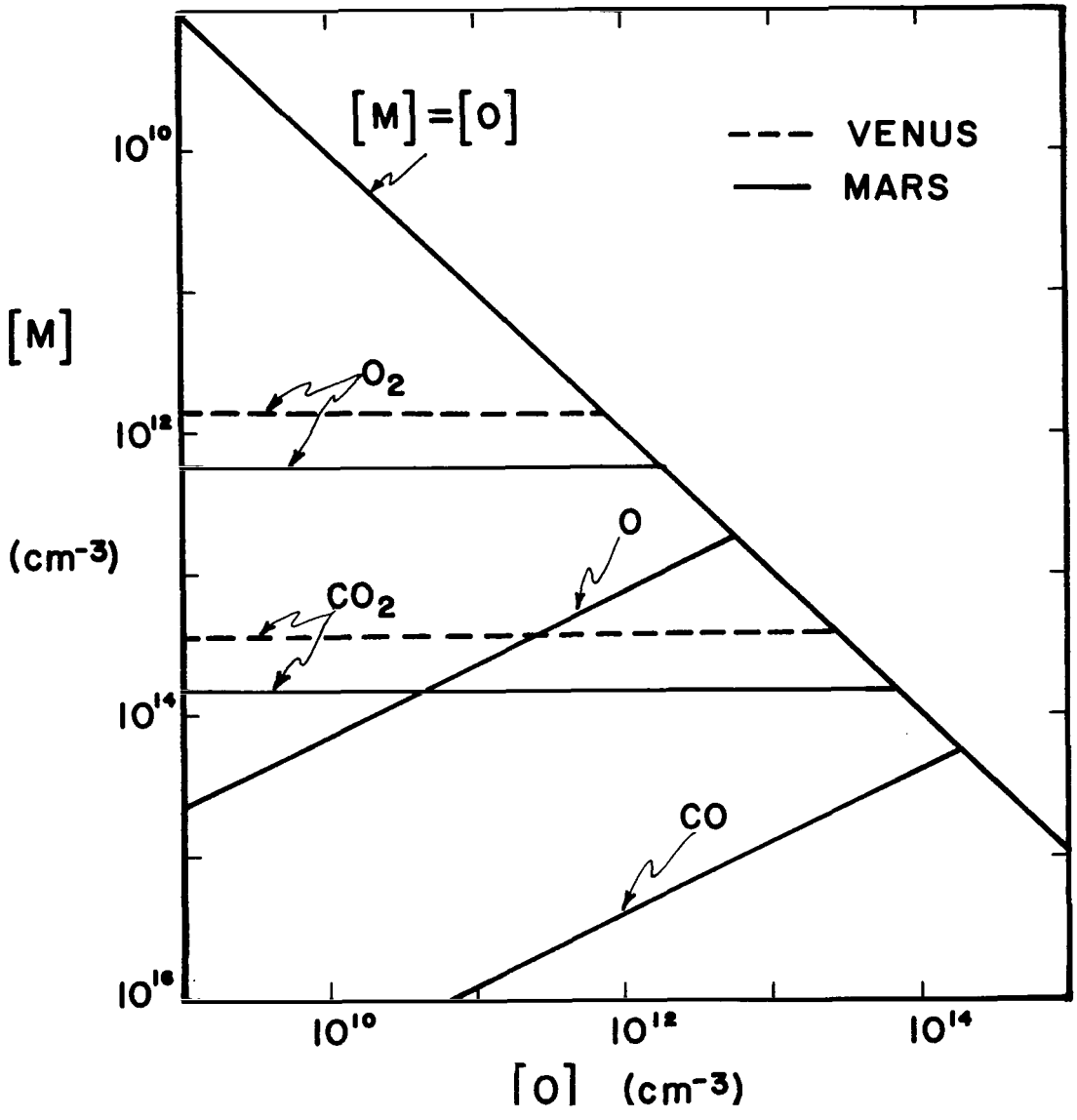

Figure 1. The area above each line specifies the total density [M] and the atomic oxygen density [O] for which the indicated constituent is in diffusive rather than photochemical equilibrium. For example, in the area bounded by the O, CO_2, and [M] = [O] lines, CO and CO_2 are in diffusive equilibrium while O and O_2 are in photochemical equilibrium.

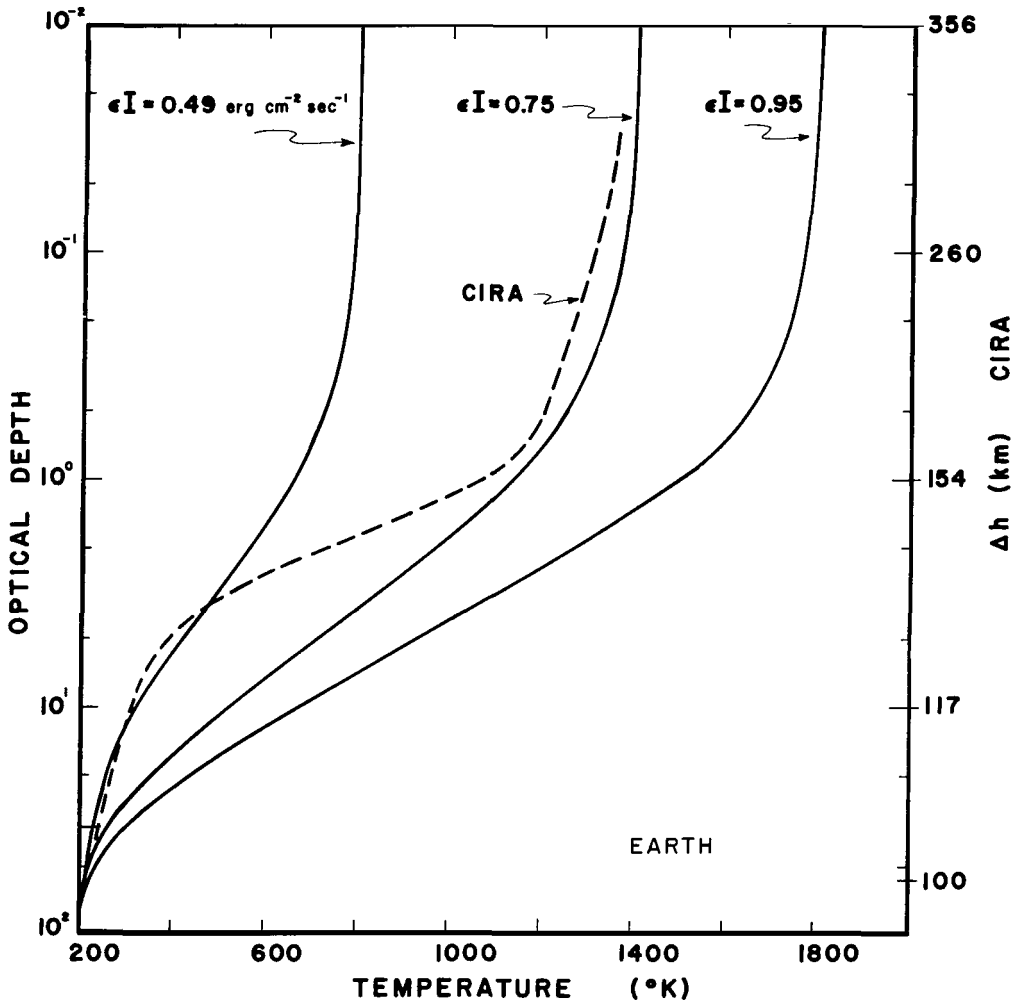

Figure 2. Temperature versus optical depth and height for the terrestrial atmosphere for maximum, minimum, and a medium sunspot number compared with CIRA 1961.

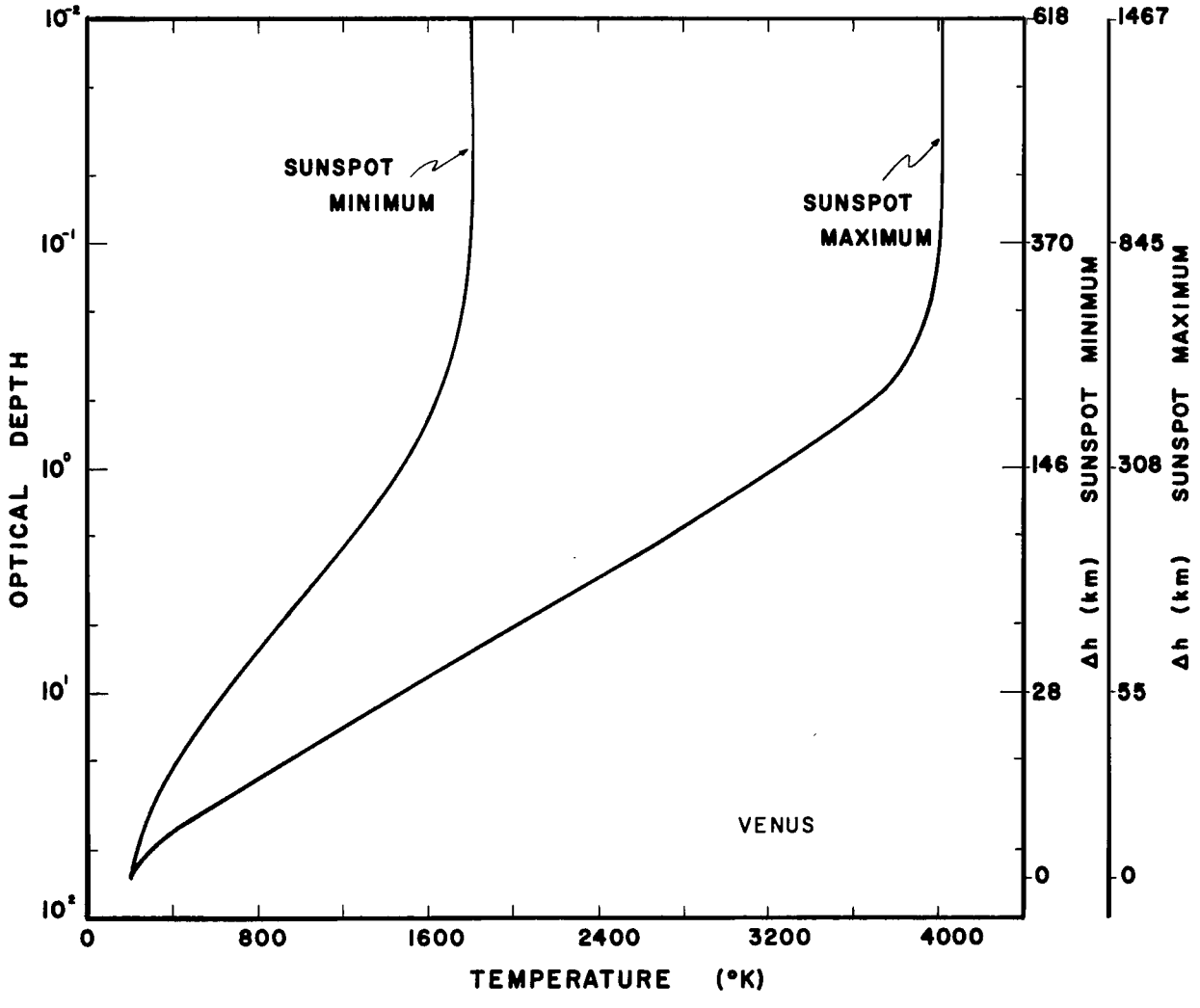

Figure 3. Thermospheric temperatures versus optical depth and height in the cytherian atmosphere for sunspot minimum and maximum.

Note: In figures 3-7 the height is measured relative to 2.3 scale heights above the occultation level.

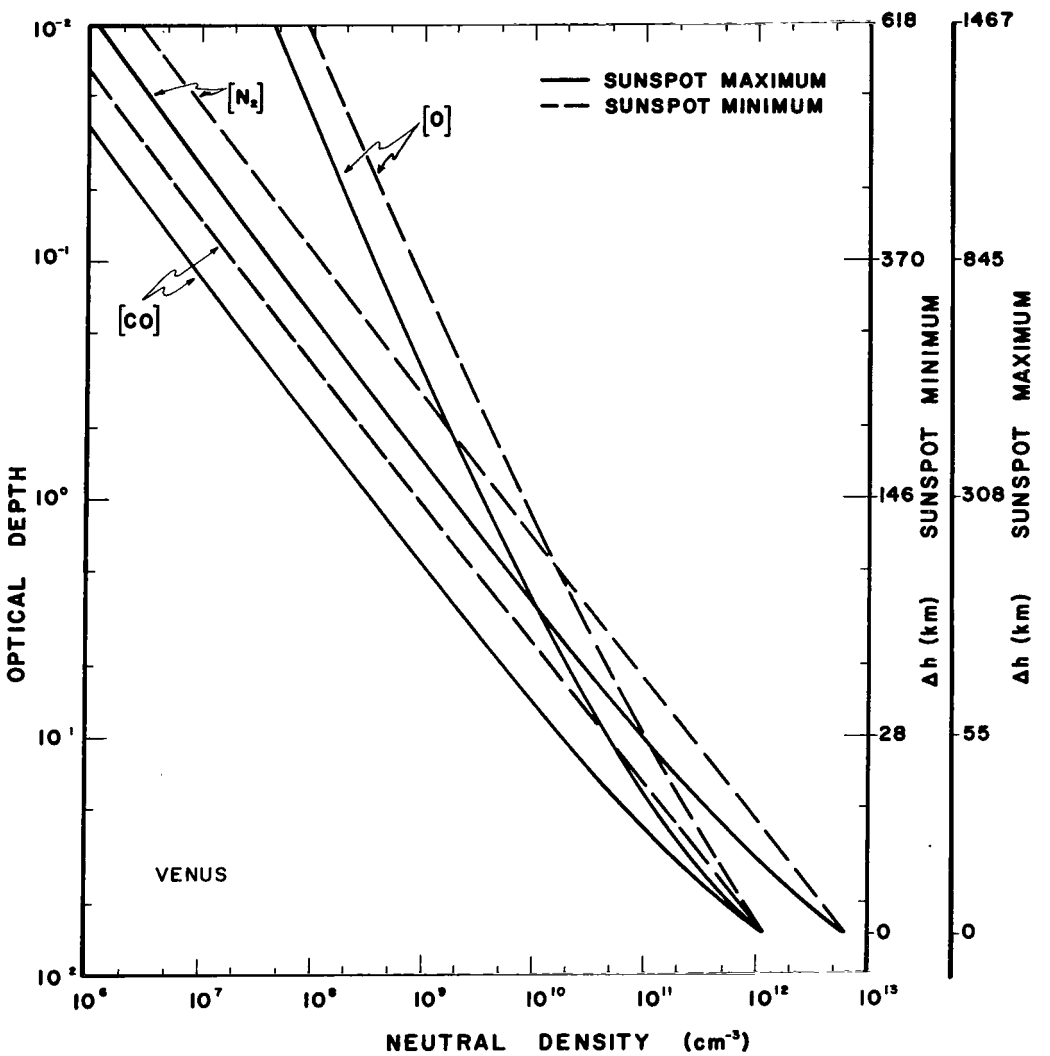

Figure 4. Neutral densities versus optical depth and height in the cytherian atmosphere for sunspot minimum and maximum.

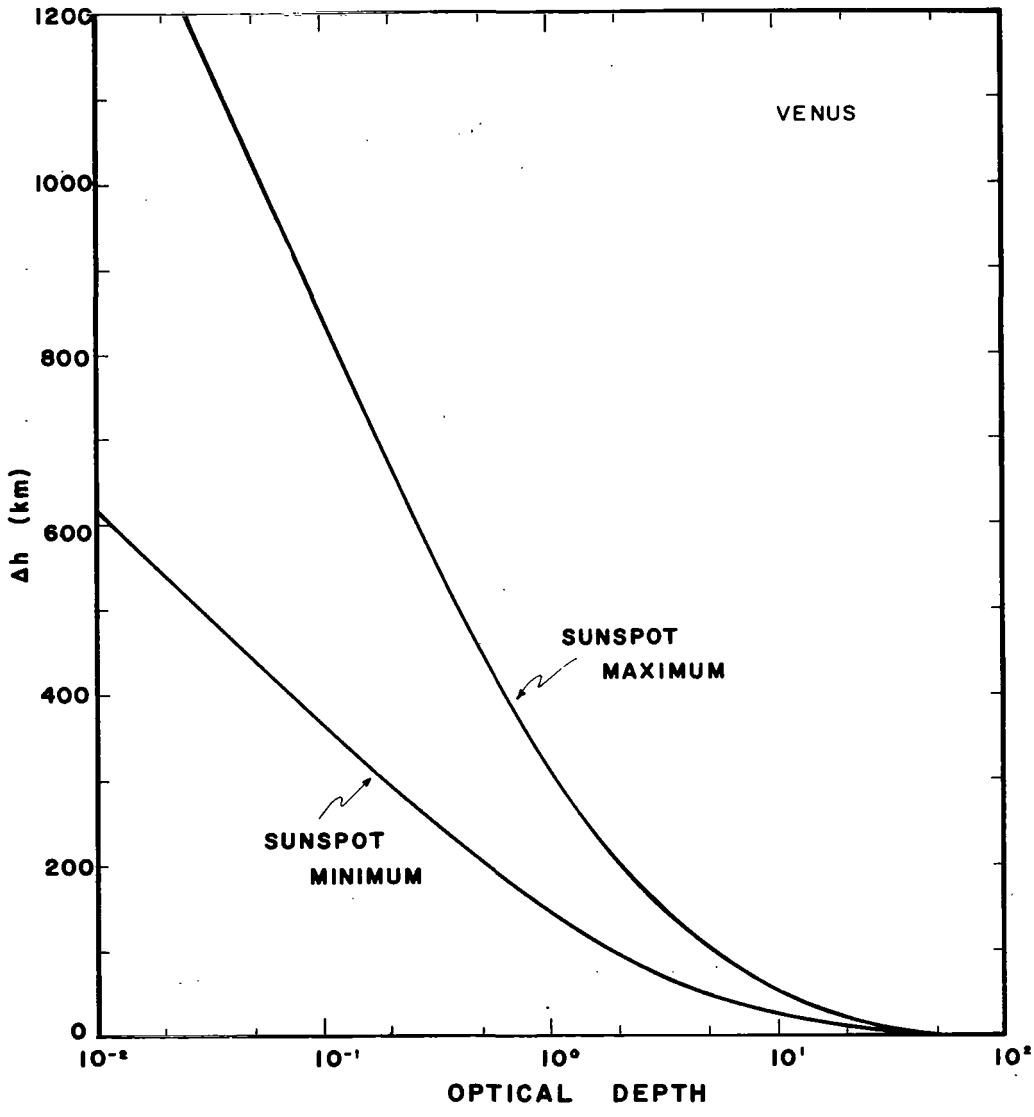

Figure 5. Optical depth versus height in the cytherian atmosphere for sunspot minimum and maximum.

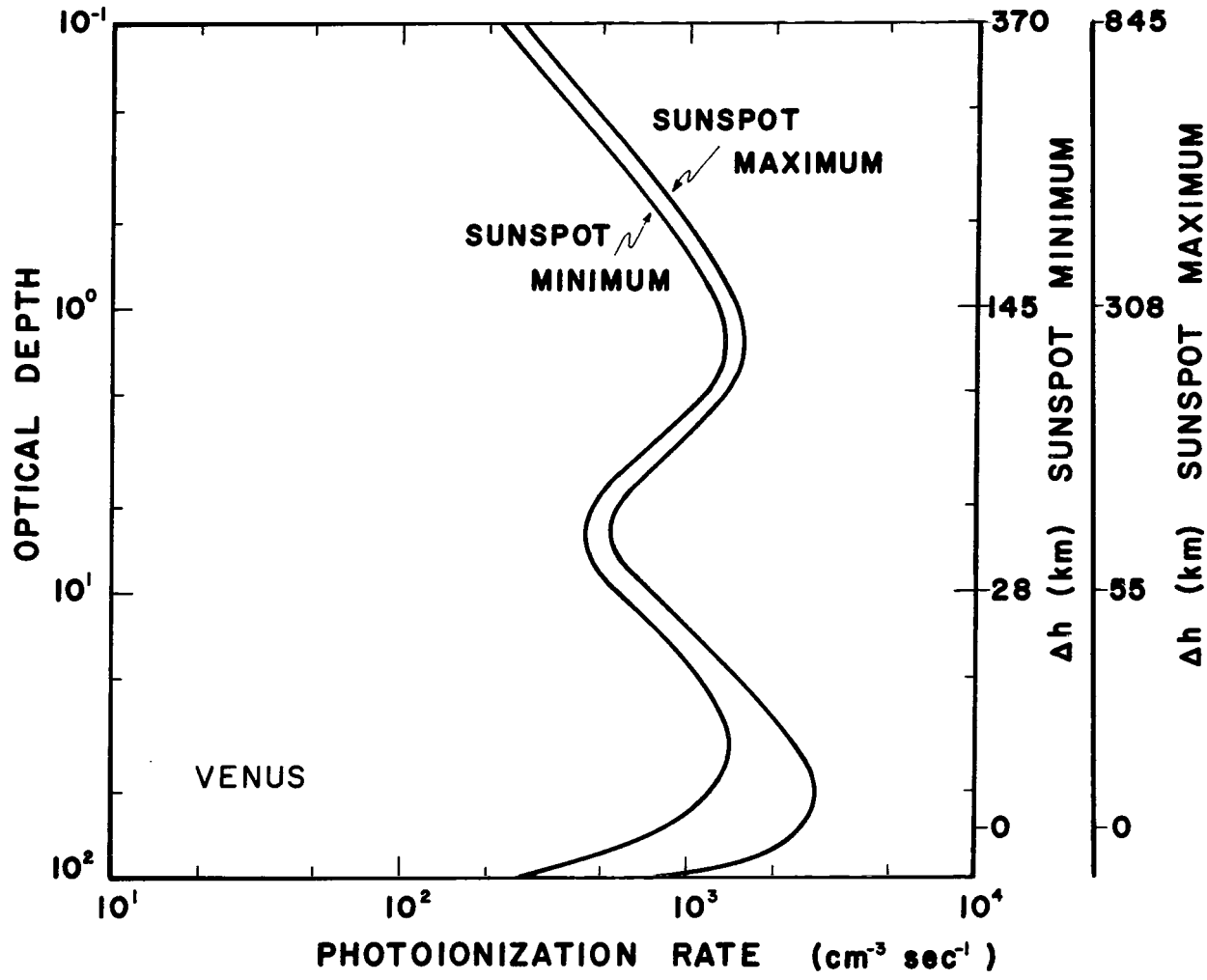

Figure 6. Photoionization rate versus height in the cytherian atmosphere for sunspot minimum and sunspot maximum.

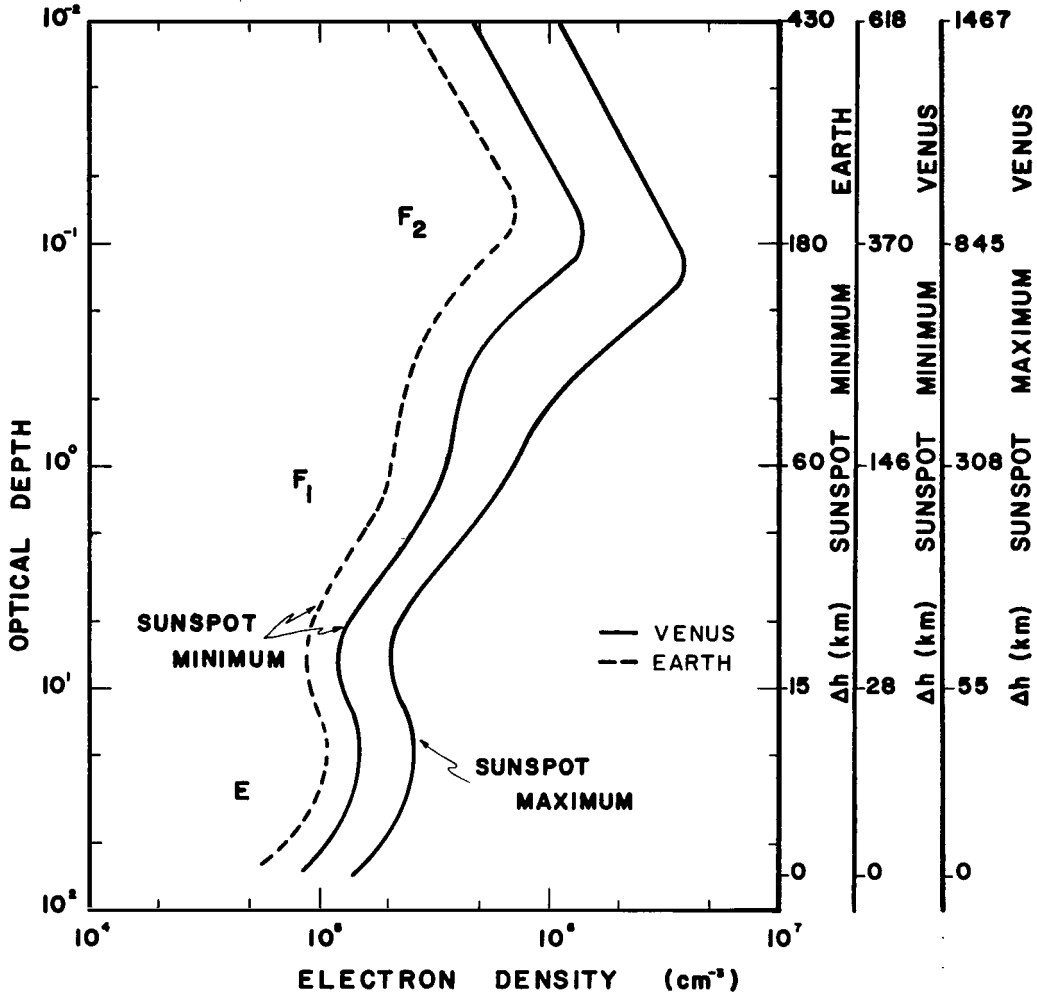

Figure 7. Electron density versus optical depth and height in the Venus atmosphere for sunspot minimum and maximum.

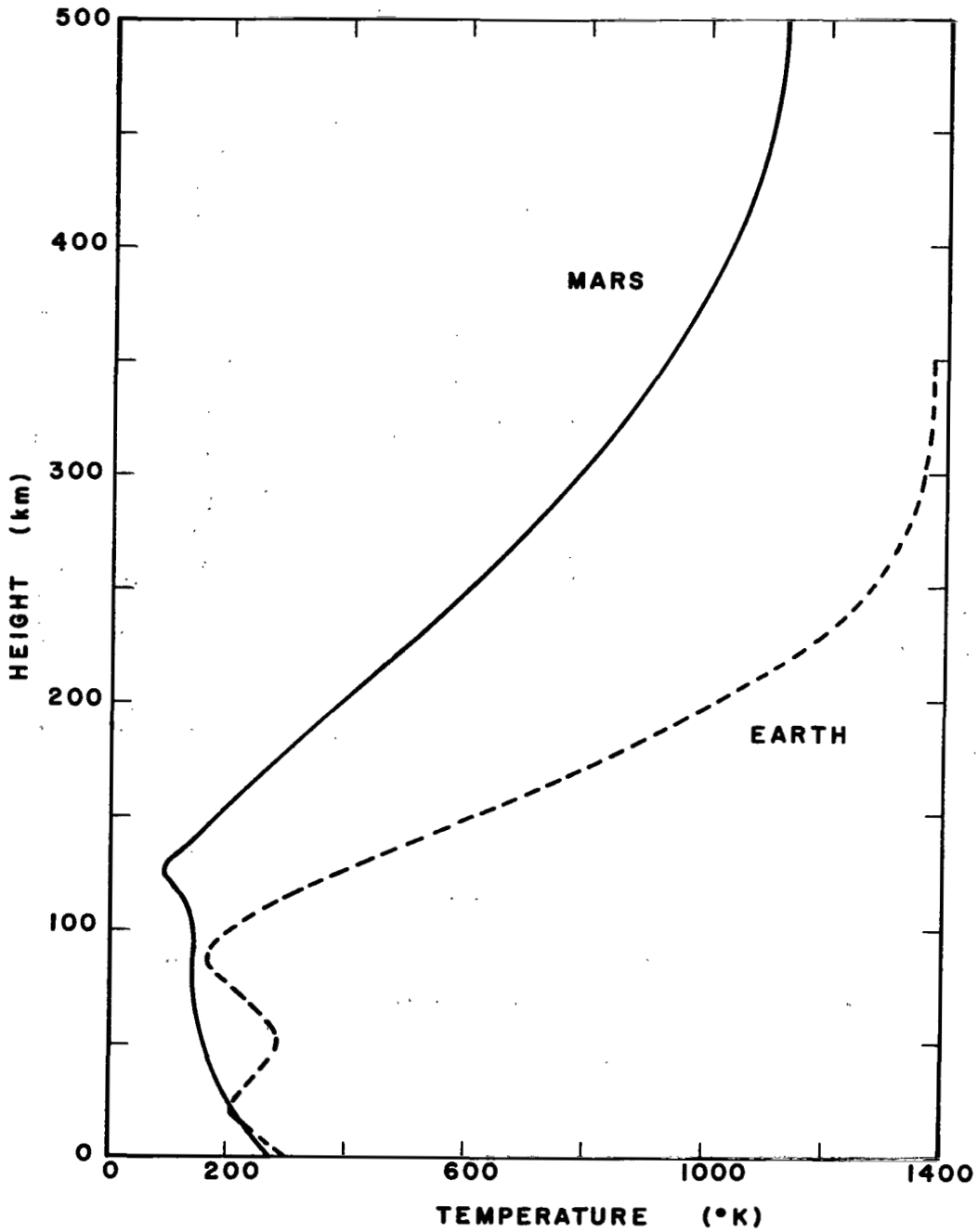

Figure 8. Temperature versus height in the martian atmosphere [Chamberlain, 1962].

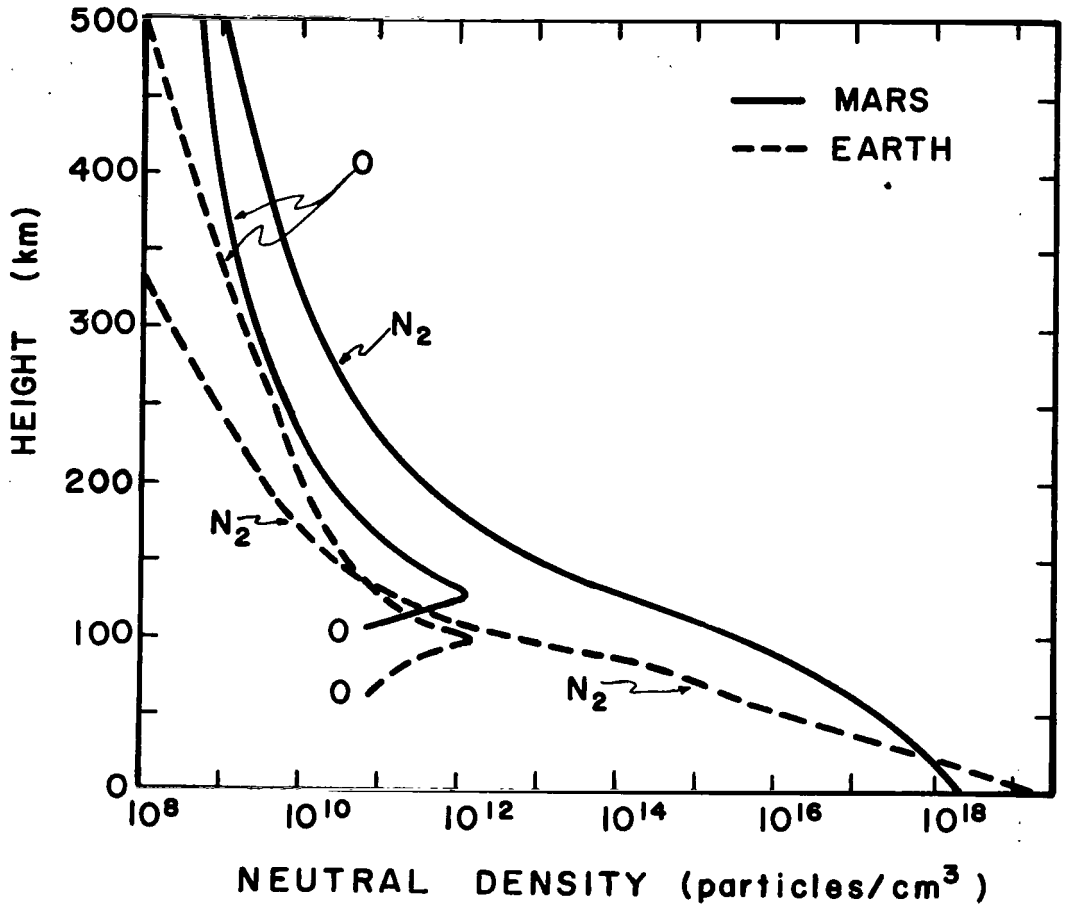

Figure 9. Neutral density versus height in the martian atmosphere [Chamberlain, 1962].

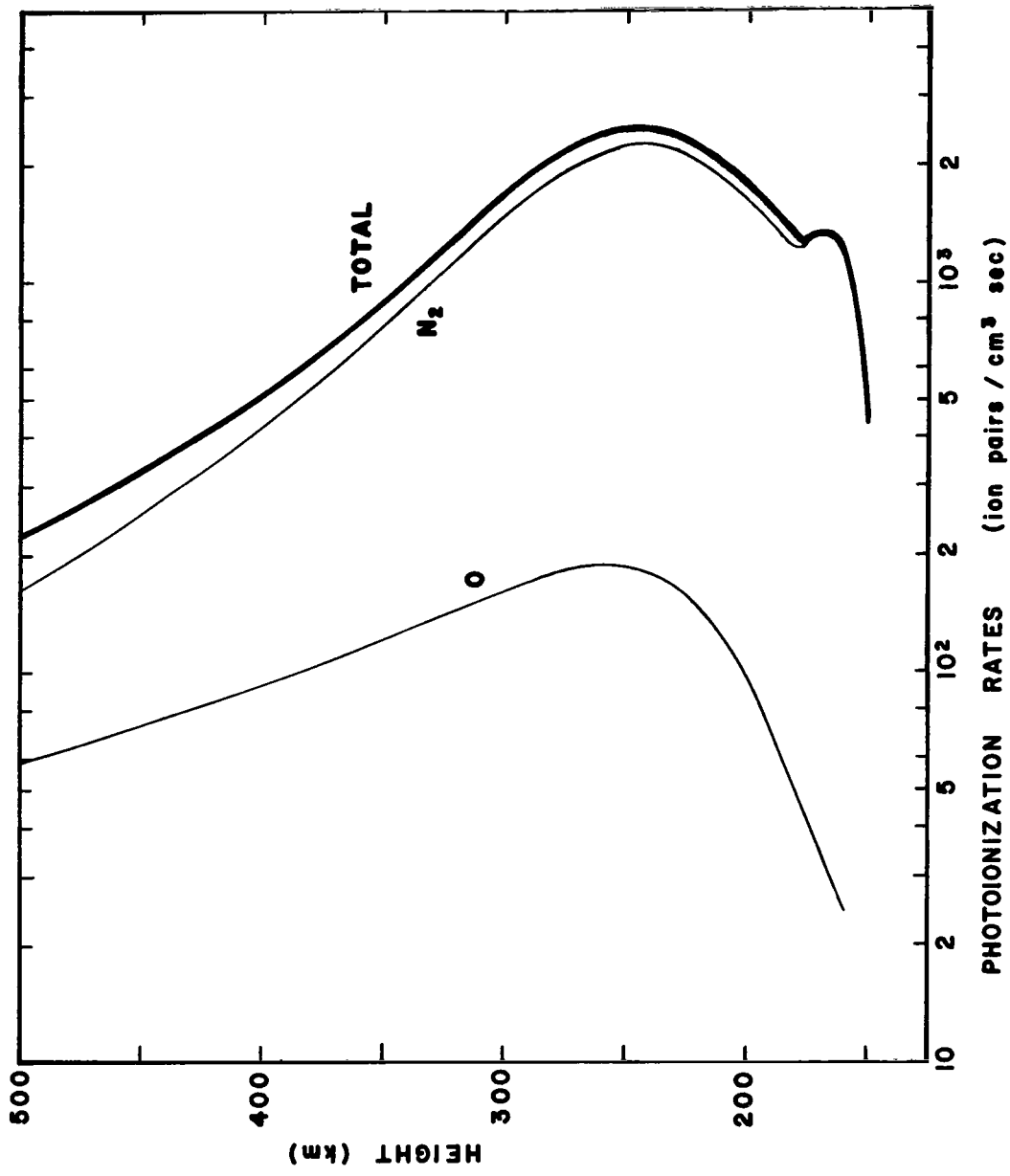

Figure 10. Ionization rates versus height in the martian atmosphere [Norton, 1963].

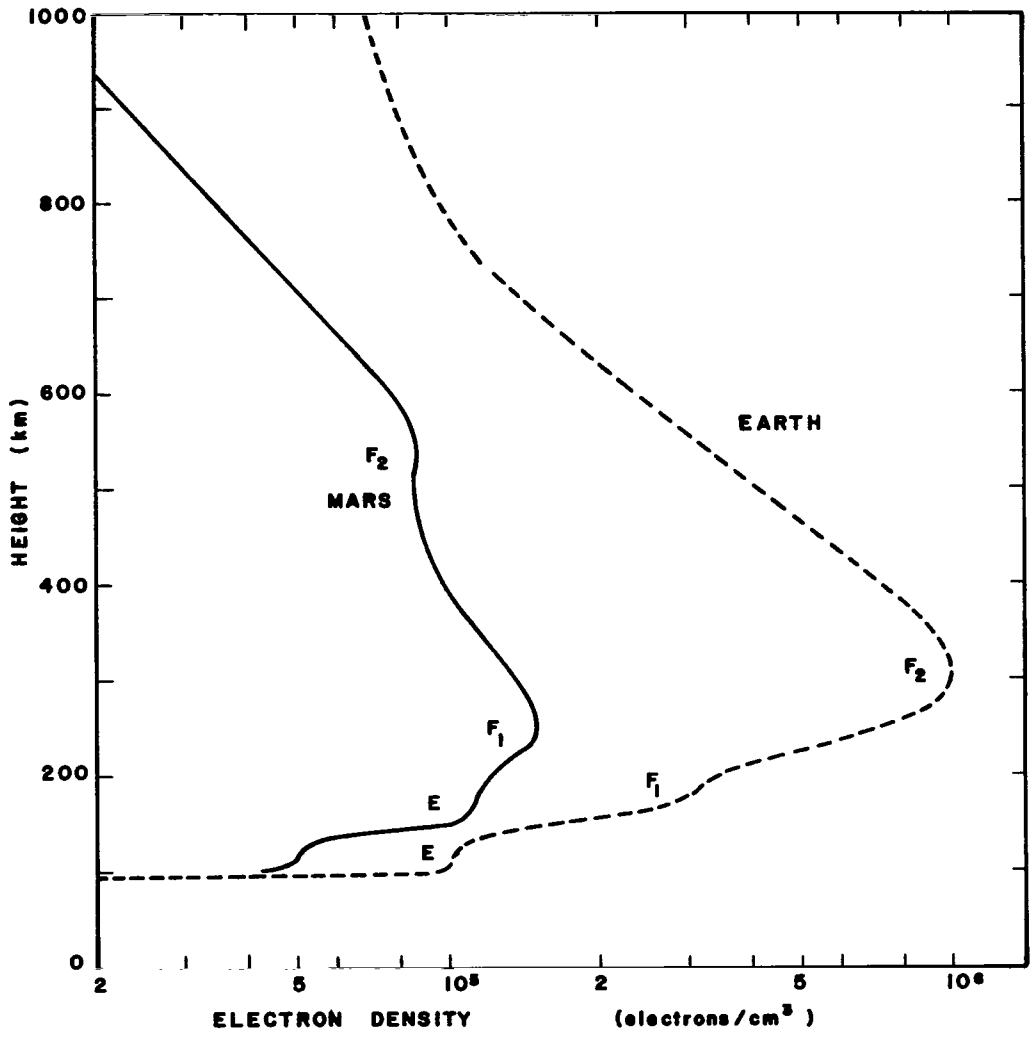

Figure 11. Electron density versus height in the martian atmosphere [Norton, 1963].

"The aeronautical and space activities of the United States shall be conducted so as to contribute . . . to the expansion of human knowledge of phenomena in the atmosphere and space. The Administration shall provide for the widest practicable and appropriate dissemination of information concerning its activities and the results thereof."

—NATIONAL AERONAUTICS AND SPACE ACT OF 1958

NASA SCIENTIFIC AND TECHNICAL PUBLICATIONS

TECHNICAL REPORTS: Scientific and technical information considered important, complete, and a lasting contribution to existing knowledge.

TECHNICAL NOTES: Information less broad in scope but nevertheless of importance as a contribution to existing knowledge.

TECHNICAL MEMORANDUMS: Information receiving limited distribution because of preliminary data, security classification, or other reasons.

CONTRACTOR REPORTS: Technical information generated in connection with a NASA contract or grant and released under NASA auspices.

TECHNICAL TRANSLATIONS: Information published in a foreign language considered to merit NASA distribution in English.

TECHNICAL REPRINTS: Information derived from NASA activities and initially published in the form of journal articles.

SPECIAL PUBLICATIONS: Information derived from or of value to NASA activities but not necessarily reporting the results of individual NASA-programmed scientific efforts. Publications include conference proceedings, monographs, data compilations, handbooks, sourcebooks, and special bibliographies.

Details on the availability of these publications may be obtained from:

SCIENTIFIC AND TECHNICAL INFORMATION DIVISION

NATIONAL AERONAUTICS AND SPACE ADMINISTRATION

Washington, D.C. 20546